

## Ultraviolet Polarized LiDAR System for Biological Aerosols

Zijian Yang, Chao Li, Feng Chen, Jiawen Mao, Taihu Wu \*

Academy Military Medical Sciences, Institute of Medical Equipment, Tianjin, 300161, China.

\* Corresponding author, E-mail: taihuwu@gmail.com

**Abstract** - Biological aerosol detection using Polarized laser remote sensing technology has the advantage of avoiding interference of strong sunlight and good accuracy. The principle is to identify different biological particles of different shapes according to different degrees of laser particle depolarization. This paper uses two 405nm laser polarization scattering detection channels to build low-power small-scale experimental telemetry device. The device uses a continuous semiconductor laser, a pseudo-random modulation and photon counting mode, with detection frequencies of 100MHz and spatial resolution of 1.5m. During the experiment, *Bacillus subtilis* and *Staphylococcus aureus* were tested as comparison targets at a distance of about 30m away from the device. The results showed that *Staphylococcus aureus* depolarization rate was about 15% higher than *Bacillus subtilis*, meaning the device can distinguish test objectives.

**Keywords** - Polarization Light Detection And Ranging (LiDAR); Bio-aerosol; T-matrix; Pseudo-random modulation

### I. INTRODUCTION

The detection and alert of bio-aerosol are very important to bioterrorism attack prevention and loss reduction. □ In contrast with traditional extraction bio-aerosol point detector, detecting optical property of bio-aerosol particle using LiDAR technique is a more cost-effective method and has become one of research hotspots in recent years. 1 According to detecting mechanism, telemetry methods of bio-aerosol can be divided into multiple signals such as Mie scattering, differential absorption, laser-induced fluorescence and polarization scattering etc. 2 Relative to other detecting methods, the Mie scattering LiDAR detects target cloud cluster by receiving elastic scattering light whose wave length is equal to light source; it has larger detection range than other equipment and has simple optical structure and strong signal to noise ratio(SNR).

Because elastic backscattering is unable to distinguish bio-aerosol particles, currently the method frequently used is to effectively distinguish biological and non-biological particles by laser-induced fluorescence. But due to weak signals of Raman spectrum, fluorescence spectrum and absorption spectrum, the method is easily interfered by various surrounding-based factors, especially background sunlight; it is difficult to distinguish between different particles with the spectrum of the method in actual application.

Therefore, the polarization approach<sup>3~5</sup> for bio-aerosol detection is under considering. At present, the T-Matrix proposed by Waterman<sup>6</sup> in 1965 is one of the widest and most effective precise theoretical calculation methods for polarization scattering specific to non-spherical particle. Its principle is to expand incident and scattered fields of light wave on the base of spherical

wave functions and to correlate its coefficient with a transition matrix. Because normalized scattering matrix is only related to particle morphology, scale parameters and relative refractive index<sup>7</sup>, T-Matrix is better than others on efficiency for free-oriented biological particle swarm.

Pal<sup>8</sup> elaborated the polarization characteristic of biological particle in 1973. After that, Mishchenko<sup>9</sup> summarized standard procedure of calculating depolarization factor of aerosol cloud using T-Matrix, and gave the calculating procedure in 1996. B.T.N. Evans<sup>10</sup> from Canada developed LiDAR scanning system based on linear depolarization factor of signal in 1994. In 2008, MIT Lincoln Lab<sup>11</sup> reported experiment results of relevant living bio-aerosol using near-infrared and far-infrared wave bands, which conformed to calculation result of T-Matrix. The American Lockheed Martin Coherent Detection Company developed a system called WANDER Lidar<sup>12</sup> based on polarization technique, achieving particle identification through combination of estimating back scattering parameter and multi-wavelength depolarization factor of target cloud.

This paper described an experiment platform for short-range standoff polarization detection using polarization scattering theory and pseudo-random modulation technology. A semiconductor continuous laser and photon counters are used for eye-safe detection. Some field trail and analysis were done based on bio-aerosol simulations including *bacillus subtilis* and *staphylococcus aureus*.

### II. PRINCIPLE OF T-MATRIX

Polarization state of a light wave can be described by the four-dimensional vector Stokes Parameter; for particle swarm, its scattered and exciting fields can be described and correlated as follows according to the Maxwell's

linear superposition principle:

$$\begin{bmatrix} I_{\text{scat}} \\ Q_{\text{scat}} \\ U_{\text{scat}} \\ V_{\text{scat}} \end{bmatrix} = \begin{bmatrix} F_{11} & F_{12} & F_{13} & F_{14} \\ F_{21} & F_{22} & F_{23} & F_{24} \\ F_{31} & F_{32} & F_{33} & F_{34} \\ F_{41} & F_{42} & F_{43} & F_{44} \end{bmatrix} \cdot \begin{bmatrix} I_{\text{inc}} \\ Q_{\text{inc}} \\ U_{\text{inc}} \\ V_{\text{inc}} \end{bmatrix} \quad (1)$$

And on the basis of Extended Boundary Condition Method (EBCM) proposed by Waterman, the backscattering matrix for free-oriented isotropic and mirror-symmetric particle swarm is as follows:

$$F(\theta = 180) = \begin{bmatrix} F_{11} & 0 & 0 & 0 \\ 0 & F_{22} & 0 & 0 \\ 0 & 0 & -F_{22} & 0 \\ 0 & 0 & 0 & F_{11} - 2F_{22} \end{bmatrix} \quad (2)$$

Consider normalized scattering matrix:

$$F(\theta = 180) = \alpha \cdot \begin{bmatrix} 1 & 0 & 0 & 0 \\ 0 & 1 - \Delta & 0 & 0 \\ 0 & 0 & \Delta - 1 & 0 \\ 0 & 0 & 0 & 2\Delta - 1 \end{bmatrix} \quad (3)$$

According to T-Matrix theory, depolarization performance of back scattering has only one parameter  $\Delta$ , which is depolarization factor. Since T-Matrix of particle is irrelevant to incident and scattered fields, depolarization factor is the characteristic value of particle as the sole parameter and can be used to distinguish morphological characteristics of particle. The Figure 1 shows how depolarization factor of isotropic and mirror-symmetric particle swarm with free orientation changes with the ratio of the horizontal to rotational axes of particles during back scattering computation using T-Matrix and Python language<sup>13</sup>. Its basic conditions for computation are: the particle diameter approximately obeys index distribution with effective radius 0.5 $\mu\text{m}$ , effective standard deviation 1 $\mu\text{m}$  and refractive index is set to be 1.52+0.01i. From the curve shape, particles with different ratios can be distinguished by the depolarization factor.

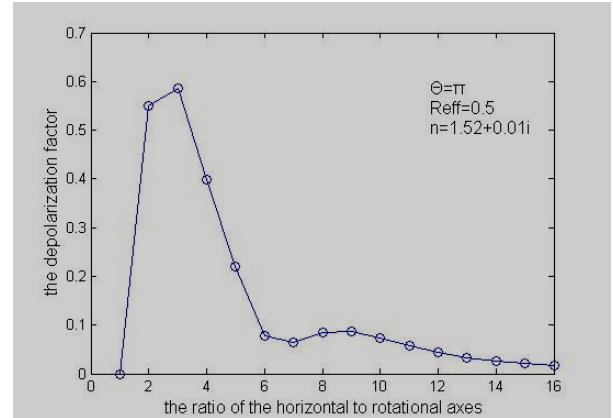


Fig. (1). Depolarization Factor Changes with Ratio of the Horizontal to Rotational Axes

### III. SYSTEM DESIGN

The original intention of system design is to develop a small telemetry platform with low power consumption. Considering that fluorescence detection channel may be added into the system in future, the excitation wavelength is set at 405nm for attempt; a semiconductor continuous laser with maximum power 100mW at 405nm produced by Coherent Company is employed. We set a linear polarizer in front of the laser head, and its polarization direction is adjusted to conform to the long axis direction of laser beam. Then the light beam is expanded to 30mm diameter and made coaxial by a set of lenses, with a divergence angle of 0.01mrad.

A Schmidt-Cassegrain telescope with the aperture of 200mm and focal length 2032mm is used as the optical receiver of the system, whose field of view is 0.02mrad. Then the signal beam is split into two mutually perpendicularly polarized beams by a 1:1 beam splitter and two analyzers. Optical paths of both polarization detection channels are equal so that both channels can be optical focused at the same time; Optical filters with the bandwidth of 405 $\pm$ 5nm are used for filtering.

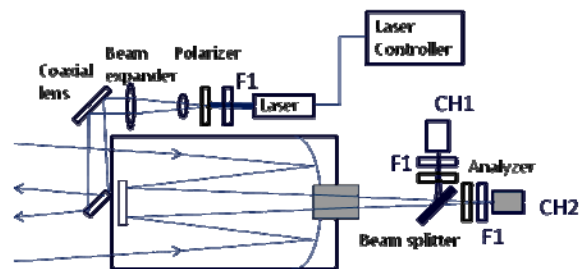
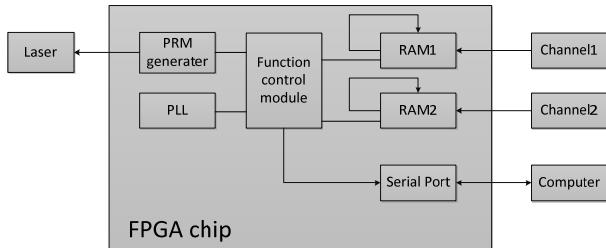


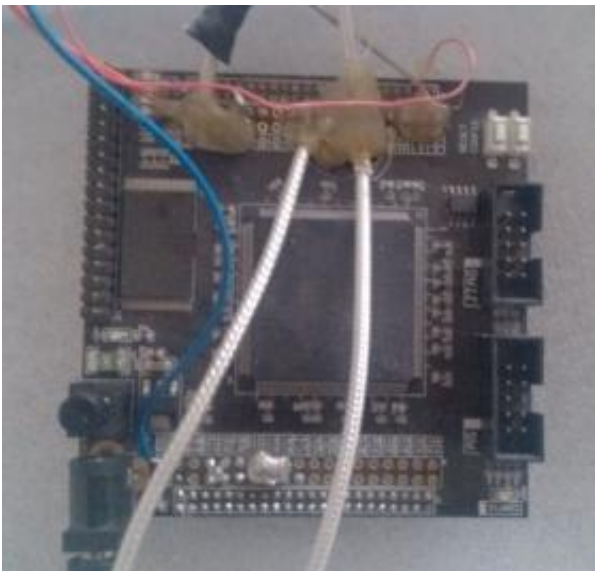
Fig. (2). Schematic of the Optic System Layout.

For detector, the platform employs the Hamamatsu H10682-210 photon counting module as detector. The first reason is that the detection ability of photon counting module is higher than that of avalanche diode and photomultiplier; the second reason is that photon counting

module outputs pulse signal with the width of 10ns and amplitude 2.2V, which can be directly input to pins of FPGA control board as digital signal, avoiding high-bandwidth A/D conversion, simplifying structure and reducing engineering difficulty.



a. Block Diagram of Real-time Acquisition Program.



b. Photo of the Capture Card.

Fig. (3). the FPGA Capture Card We Used.

The platform uses an FPGA chip for actuating laser pulse and recording detection signal. At first, the FPGA chip modulates laser pulse signal circularly with the frequency of 100MHz using a pseudo-random code at the length of 255. Output power of the whole laser source is about 50mW. At the same time, the system collects output pulse of the two detection channels respectively by two two-port RAMs simulated by the FPGA chip at the frequency of 100MHz. Then the chip computes and superimposes the corresponding spatial signal in real time. The spatial resolution of the system is 1.5m and theoretical maximum detecting range is 382m. For the demands of high-speed response and real-time processing, all computing and controlling modules are simulated within the FPGA chip to keep the response speed of electric circuit not lower than 10ns. Data collected each

frame is transmitted to upper computer via serial port for further analysis and display.

The characteristic of pseudo-random modulation is that its autocorrelation function is similar to a  $\delta$ -function, convenient to modulate and demodulate and with high detection rate. By achieving modulation of continuous laser, it does not only lower the requirement for instantaneous power of laser, but also makes receipt signal count evenly distributed in the ram, fully utilizing chip resources.

The SNR for pseudo-random modulation LiDAR is<sup>14</sup>

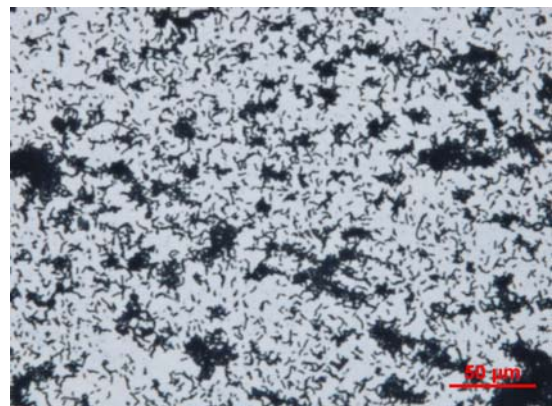
$$SNR_{PRM} = \frac{\sqrt{M} \sqrt{E} I P_0 G_j}{\sqrt{I P_0 G + 2b}} \quad (4)$$

where M represents the accumulation period, l represents the number of pulses emitted each cycle, G<sub>j</sub> represents the signals, b represents the background noise, P<sub>0</sub> represents the energy corresponding to each code. A pulse LiDAR can be considered as a pseudo random modulation radar with l=1. Comparing the SNR of pulsed excitation and pseudo-random excitation through computation, the SNR of pseudo-random modulation is weaker than pulse modulation under the same pulse energy excitation under high background noise. That is why we choose the length of pseudo-random code 255. Hence, we prefer increasing the number of cycles to longer pseudo-random code each cycle.

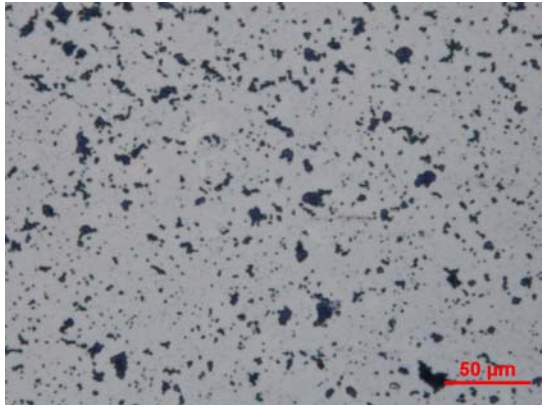
#### IV. EXPERIMENTAL RESULTS

To compare the difference of bacterial morphological, the experiment is planning to use bacillus subtilis and staphylococcus aureus as study subjects.

First the bacteria samples were observed with an optical microscope. Both samples are gram-stained at first, then their cytoderm morphology is observed with 400X optical microscope; the result is as shown in Figure 4, the size of bacillus subtilis is about 0.7~0.8×2~3um, while staphylococcus aureus is about 0.8um.



a. Bacillus Subtilis



b. Staphylococcus Aureus

Fig. (4). Shape Observation of Gram Staining Bacteria under an Optical Microscope.

Bioaerosol at approximately  $10^6$ ppf consisting of wet bacillus subtilis and wet staphylococcus aureus was generated in the air by an aerosol generator as test targets of the LiDAR system. The experiment was conducted under dark background (Beijing Time 20 : 00~23:00), with the temperature of 5°C and relative humidity 30%.



Fig. (5). Photo of the Lidar System in the Field Tests.

Due to scale limitation of the experiment site, an OD2 attenuation slices are added at each scattering channel to adjust scattering light intensity. The system successively detects pure water aerosol, bacillus subtilis aerosol and staphylococcus aureus aerosol for 5 times respectively at the distance of about 30m, taking sky as background. Figure 6 shows one certain raw signal detection.

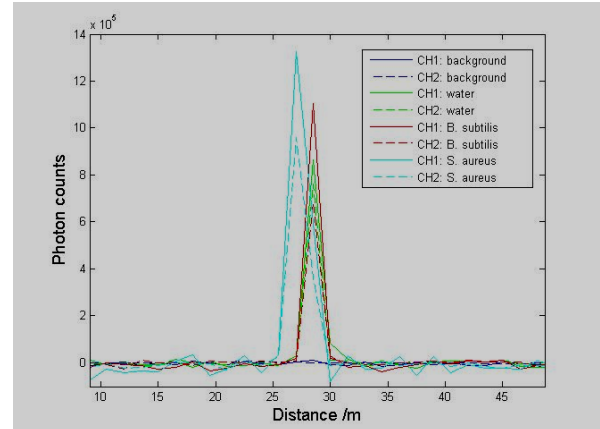


Fig. (6). The Raw Data Signal

The five results are analyzed; the differences between peaks and baselines of signals are regarded as effective signals. Figure 7 shows the results.

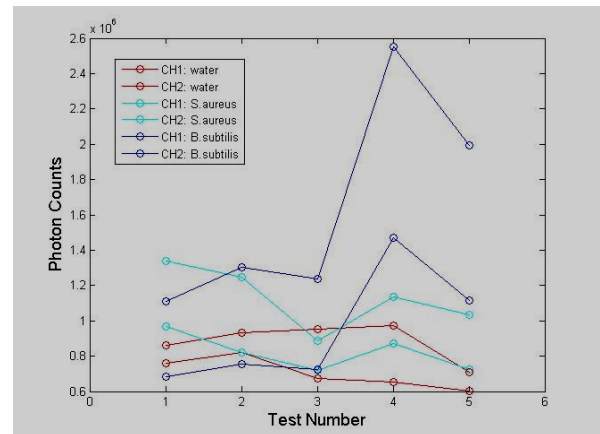


Fig. (7). the Results of 5 Measurements

Depolarization factor  $\Delta$  is calculated on the basis of above detection results; the results are shown in Figure 8.

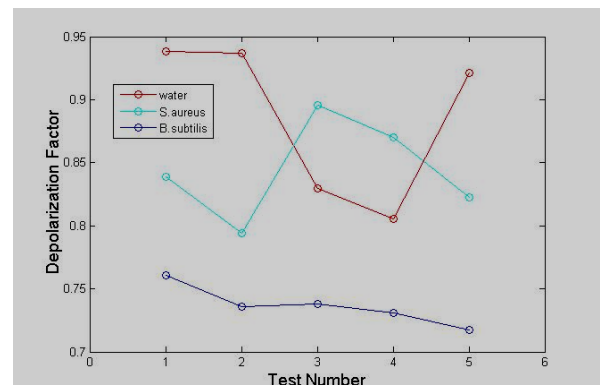


Fig. (8). the Depolarization Factor of the 5 Measurements

Since depolarization factor has many definitions, the calculation this paper employs is as follows:

$$\Delta = \frac{I_{\perp}}{I_{\parallel} + 2I_{\perp}} \quad (5)$$

Figure 8 shows that the depolarization factor is higher than simulative calculation data, which may result from refractive index set and shape parameter deviation, or interference of background noise when detecting. Mean depolarization factor for detecting water, bacillus subtilis and staphylococcus aureus are 0.8861, 0.8441 and 0.7366 respectively where the depolarization factor of staphylococcus aureus is about 15% higher than that of bacillus subtilis. The depolarization factor of the spherical staphylococcus aureus is close to that of pure water aerosol but significantly different from that of the bacilliform bacillus subtilis because pure water keeps spherical in air due to its own tension. Here the depolarization factor of water and staphylococcus aureus is not zero as simulated just because the real particles are not standard spherical but with a small ratio of the horizontal to rotational axes. The result indicates that the telemetry using pseudo-random modulation of ultraviolet laser can distinguish different bio-aerosol particles according to their polarization factors.

As the limitation of test site, we did not measure the detective distance it covered. But it could be calculated according the LiDAR equation in which the signal is inversely proportional to square of the distance. So the platform could work at about 300m without the OD2 attenuation slice.

## V. CONCLUSIONS AND PROSPECT

Compared with laser-induced fluorescence, bio-aerosol detection using polarization scattering may overcome sunlight interference and cover a longer distance. This paper conducts a telemetry platform with two orthogonally polarizing backscattering detection channels, and some experiment results about the bio-aerosol distinguishing between bacillus subtilis and staphylococcus aureus. The result shows that depolarization factor of the two bacteria is significantly different, where the depolarization factor of staphylococcus aureus is about 15% higher than that of bacillus subtilis, and the system could realize its function as far as 300m theoretically. Therefore, particle type can be distinguished with this method.

Since back scattering cross-section of bacteria is two to three orders of magnitude larger than fluorescence scattering, detection using scattering light has certain advantages on detection range. But because of low distinction degree of depolarization factor for different particles, higher detecting precision of polarization scattering is required. In the next work, we will improve the detection sensitivity and try whether other methods

such as fluorescence detection can be combined with for cross validation and a higher resolution.

## CONFLICT OF INTEREST

The authors confirm that this article content has no conflicts of interest.

## ACKNOWLEDGMENT

This work is supported by the National Twelfth Five major project (No. AWS11Z005-4), China, and the National Science and Technology Major Project (No. 2012ZX10004801), China.

## REFERENCES

- [1] Primmerman, Charles A. "Detection of biological agents." *Lincoln laboratory journal* 12.1 (2000): 3-32.
- [2] Buteau, S., et al. "Final Report for Task Group (RTG-55) on Laser based stand-off detection of biological agents." *NATO RTO SET098 TG55 final report, 76pp* (2008).
- [3] WEI, Pei-yu, et al. "Nonspherical Model for Biological Aerosol and Its Application to the Research of Unpolarized Light Multiple Scattering." *The Journal of Light Scattering* 2 (2013): 004.
- [4] Brown, Andrea M., et al. "Models to support active sensing of biological aerosol clouds." *SPIE Defense, Security, and Sensing. International Society for Optics and Photonics*, 2013.
- [5] Thrush, Evan, et al. "Backscatter signatures of biological aerosols in the infrared." *Applied optics* 51.12 (2012): 1836-1842.
- [6] Waterman, P. C. "Matrix formulation of electromagnetic scattering." *Proceedings of the IEEE* 53.8 (1965): 805-812.
- [7] Nicolet, M., M. Schnaiter, and O. Stetzer. "Circular depolarization ratios of single water droplets and finite ice circular cylinders: a modeling study." *Atmospheric Chemistry and Physics* 12.9 (2012): 4207-4214.
- [8] Pal, S. R., and A. I. Carswell. "Polarization properties of lidar backscattering from clouds." *Applied optics* 12.7 (1973): 1530-1535.
- [9] Mishchenko, Michael I., Larry D. Travis, and Daniel W. Mackowski. "T-matrix computations of light scattering by nonspherical particles: A review." *Journal of Quantitative Spectroscopy and Radiative Transfer* 55.5 (1996): 535-575.
- [10] Evans, B. T. N., et al. "Remote detection and mapping of bioaerosols." *Journal of aerosol science* 25.8 (1994): 1549-1566.
- [11] Richardson, Jonathan M., John C. Aldridge, and Adam B. Milstein. "Polarimetric lidar signatures for remote detection of biological warfare agents." *SPIE Defense and Security Symposium. International Society for Optics and Photonics*, 2008.
- [12] Carrig, Timothy J., Christian Grund, and John Marquardt. "Wavelength normalized depolarization ratio lidar." *U.S. Patent No. 7,339,670*. 4 Mar. 2008.
- [13] Leinonen, Jussi. "High-level interface to T-matrix scattering calculations: architecture, capabilities and limitations." *Optics express* 22.2 (2014): 1655-1660.
- [14] Takeuchi, N., et al. "Random modulation cw lidar." *Applied optics* 22.9 (1983): 1382-1386.